Design of an anechoic termination for an open ended duct

Thomas Finlay (1), Orddom Leav (1) and Stephen Moore (1)

(1) Defence Science Technology Group, 506 Lorimer Street, Port Melbourne 3207, Victoria, Australia

Anechoic terminations of ducts are used in acoustic testing platforms, such as specified in ISO 5136, to reduce the effect of acoustic waves reflected at the outlet from impacting the characterization of test specimens. In cases where duct elements are characterized in the presence of flow, the anechoic termination must not impose a significant flow restriction. In ISO 5136, an anechoic termination with an open outlet is required and the standard recommends designs for the anechoic termination. However, there is very little background or references provided in the standard to justify the anechoic termination design. This paper investigates the effect of different outlet geometries and lining materials on the outlet reflection coefficient for no flow in the duct. A finite element model is developed using COMSOL software and validated against analytical models of unflanged open ended ducts, before being used to find reflection coefficients for different outlet conditions. These different outlet geometries include conical and catenoidal horns. A poroacoustic liner is added to the diverging section of the horns to investigate the effects of different materials. A general relationship between the relative horn size and reflection coefficient is found for each case, with the effect of poroacoustic liners found to be very important in minimizing reflection coefficient. Horns truncated in diameter are also modelled and results show that horn truncation can improve the anechoic response over a wide frequency range. The research provides a numerical framework for developing an anechoic outlet that can be used in systems where flow is present.

1 INTRODUCTION

An anechoic termination is used at the end of ducts to absorb outgoing acoustic energy and minimise reflections. This is particularly useful when investigating the acoustic properties inside ducts, where properties such as sound power, impedance, reflection coefficient and transmission loss can be found by measuring the in-duct acoustic pressures. While investigations of ducts without flow conditions can be completed using a traditional anechoic termination such as foam wedges, once flow is added, the use of these terminations is not possible. This calls for the development of a termination which both allows for flow and is anechoic.

Such terminations have been developed in the heating, ventilation and air conditioning (HVAC) industry, for measurement of sound power emitted by fans, as described in ISO 5136 (ISO5136:2003, 2003). Within ISO 5136 there are different designs that can be used for the anechoic termination to achieve a desired reflection coefficient. The theory guiding the design of these terminations is that there is an enlargement of the outlet such that it provides a gradual impedance change to match the outlet impedance. Additional attenuation is provided by including a poroacoustic lining, while maintaining the internal cross-section area of the duct to minimise flow disturbances.

As highlighted previously, ISO 5136 recommends a diverse range of designs for the anechoic termination, but the largest deviation in the designs is in the geometry. One of the preferred geometries presented in the standard is an axisymmetric catenoidal horn, which has benefits over the traditional exponential horns. The gradual change in geometry for the catenoidal horn presents preferable impedance changes for minimising reflections, when compared against an exponential horn. An example where axisymmetric catenoid horns was implemented is in early work by Bolleter et al. (Bolleter, Cohen, & Wang, 1973) for in-duct sound power measurement and has shown good performance. Donkin (Donkin, 2020) has designed and implemented the axisymmetric catenoidal

horn based on the dimension in ISO 5136 and has demonstrated excellent performance in minimising the reflection coefficient that meets the design requirements in ISO 5136. Myers (Myers, 2012) investigated the reflection coefficient of catenoidal horns with no poroacoustic lining, but at the mouth of the horn there is a straight duct section that is lined with a poroacoustic lining. The work by Myers (Myers, 2012) involved developing analytical models for designing anechoic terminations, which were validated against experimental results. Another popular design used for anechoic termination recommended by ISO 5136 is the design by Wollher (Wollherr, 1973), and later modified in works by Neise and Arnold (Neise & Arnold, 2001) and Xin et al. (Xin, Yang, Jing, & Sun, 2018), which consists of constant width prism sections with a gradual increase in height. These prisms are designed in sections and contain a duct with constant cross section surrounded by a poroacoustic lining with large voids. The design of Xin et al. (Xin, Yang, Jing, & Sun, 2018) attempts to incorporate the catenoidal design in the outlet with the poroacoustic material and partitions forming the shape of the catenoid as a prism. The geometry provides adequate reductions in reflection coefficients, and has good agreement with numerical models for frequencies between 400-1000 Hz.

From the literature survey there is limited work investigating the design for axisymmetric catenoidal horns for anechoic end terminations. With numerical simulations, this research seeks to better understand design decisions made when choosing the geometry for axisymmetric anechoic termination, and briefly investigates different materials which could be used in the construction. The paper first discusses the methodology and computational domain for the numerical simulations. Following this, results are presented for two different horn geometries, a conical horn and catenoidal horn. Attenuation by the poroacoustic lining in a conical horn is investigated by varying the static air-flow resistivities in the poroacoustic material model. Finally, the results are summarised in the conclusion section.

2 METHODOLOGY

2.1 Reflection coefficient as a performance metric

An important concept in the design for anechoic outlets is the reflection coefficient which can be measured by the ‘two-microphone method’. Munjal (Munjal, 2014) provides a comprehensive review of the two-microphone method which finds acoustic properties such as the reflection coefficient as a function of axial position along a duct using transfer function, H_{21}:

$$H_{21} = {p_2}/{p_1} \tag{1}$$

where p, is the acoustic pressure, subscript 1 denotes the microphone upstream and subscript 2 denotes the microphone downstream. The acoustic pressures are harmonically-varying quantities with a time dependence, $e^{i\omega t}$, where i is a complex number, ω is the angular frequency, and t is time. Furthermore, the method assumes that there is only acoustic plane wave propagation, and we are below the cut-on frequency.

Using the transfer function, the reflection coefficient for the case of no flow can be determined using the following:

$$R_c(l) = \left\{\frac{H_{21}-e^{-iks}}{e^{iks}-H_{21}}\right\} e^{2ikl} \tag{2}$$

where $k = \frac{2\pi f}{c}$ (wave number), f is the frequency, c is the speed of sound, l is the distance between microphone 1 and the termination, and $s = |z_1 - z_2|$ is the distance between microphones. For the purpose of this work, the speed of sound is 343 m/s and the density is 1.20 kg/m^3. It should be noted that for a perfectly reflecting terminations, $R_c = 1$, while for a perfectly anechoic termination, $R_c = 0$. Munjal (Munjal, 2014) also highlights the effects of microphone spacing on the high frequency limits:

$$s < \frac{c}{2f_{max}}. \quad (3)$$

2.2 Computational setup

The system was numerically modelled using a commercial Finite Element Analysis (FEA) package, COMSOL. The simulations solved the linearised acoustic wave equation (Helmholtz equation) for the acoustic pressure. The model assumes that the medium is a homogenous fluid (air), is compressible, and the perturbation in acoustic pressure is small compared to the mean pressure. Furthermore, for simplicity the study assumes that the medium is stationary with no fluid flow, and temperature is assumed to be constant. Future work will investigate the effects of flow and temperature on the reflection coefficient.

Figure 1 shows a schematic of the computational domain, where the 2-D axisymmetric duct and poroacoustic liner geometry was adapted for each case to reduce the computation time compared to full 3-D studies. This was necessary due to the large number of geometries and frequencies explored. Figure 1a shows an acoustic source at the base of the domain that is constrained in a straight duct with rigid walls and has diameter $d = 0.05$ m. The red dots indicate the position of the microphone pair used to calculate the reflection coefficient of the outlet; the spacing was,

$$\frac{0.9c}{f_{max}} = 0.0702 \text{ m}, \quad (4)$$

which meets the requirement set by Equation 3. The expansion at the outlet is constrained with a rigid wall and the interior surface is lined with a poroacoustic material that fills the volume between the conical or catenoidal horn and an axial projection of the straight duct. The poroacoustic lining is modelled in COMSOL using the single parameter, static airflow resistivity, poroacoustic Miki model. There is an intermediate domain for the sound to propagate before the acoustic waves are attenuated by perfectly matched layer (PML) elements. The numerical domain's height and width was adjusted with the horn's size to maintain a consistent ratio between the horn's length and the distance to the domain's edge, as per mesh independence studies.

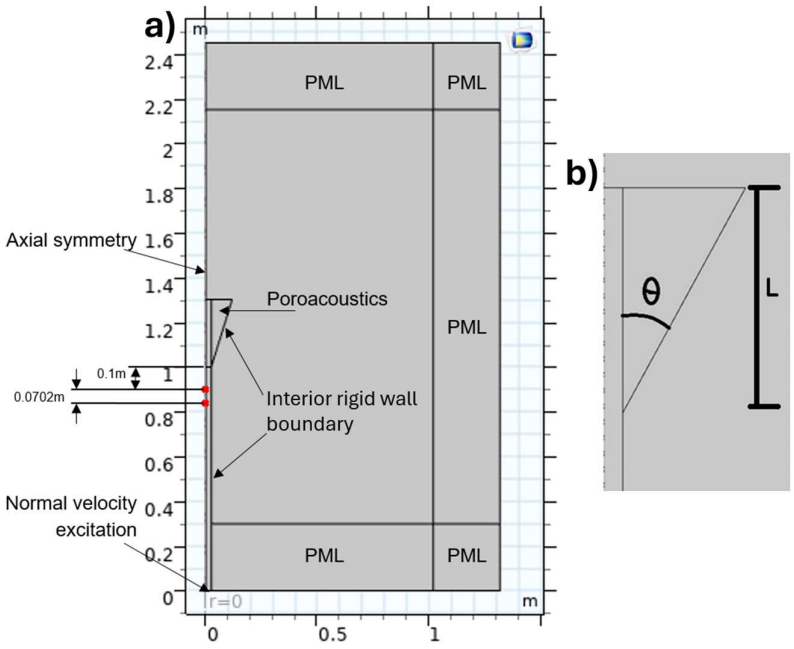

Figure 1a) Domain setup (Conical), PML is perfectly matched layer. All in duct region and free space around duct and horn are defined by pressure acoustics. Microphone locations in red. b) Angle and length definition for conical horn.

In the numerical simulations two different materials were used in the Miki models: glass wool and Durablanket, with airflow resistivities of 1424.2 kg/(m³·s) and 79800 kg/(m³·s), respectively. The airflow resistivity properties of the glass wool were provided in a COMSOL poroacoustic tutorial (COMSOL, n.d.) and the air flow resistivity value for a ceramic fibre blanket, Durablanket, was measured by the University of Adelaide using a Mecanum airflow resistivity meter. ISO 5136 does not state a static airflow resistivity in defining the liner to be used in the design of an axisymmetric catenoid shaped anechoic termination, however it does mention the use of multiple materials: fibre glass or open cell foam with a density of 24 kg/m^3 for the catenoid and fibre glass with a density of 48 kg/m^3 for the annular section (ISO5136:2003, 2003).

Catenoidal horns were also investigated as literature suggests it to be an effective geometry for minimising the reflections when designing anechoic terminations (Myers, 2012). Catenoidal horns may be parametrised by their length and diameter which are used in determining a flare factor m for input to a hyperbolic function.

$$m = \frac{1}{x} acosh\left(\frac{d_2}{d}\right), \tag{5}$$

$$D_c = cosh(mx), \tag{6}$$

where d_2 is the horn mouth diameter, d is the horn throat diameter, and x is the axial position from the throat of the horn. Parametric studies for length and mouth diameter of the catenoidal horn were completed.

In order to validate the method for calculating reflection coefficient ($\mathcal{R}$) and validate numerical FEA for the simulations, a straight duct with different end boundary conditions was modelled. This was completed with both a PML section and a rigid wall or end cap at the end of a duct for a frequency range of 0 to 1000 Hz. These results satisfied expectations and agreed with theory.

The next simulations were of an unflanged circular duct. Silva et al. (F. Silva, 2009) gives empirical relations for reflection coefficients, that fit results from the analytical work derived by Levine and Schwinger (Levine & Schwinger, 1948) and were used to validate the numerical results. Figure 2 shows a comparison of the numerical simulation against the approximation by Silva et al. (F. Silva, 2009), and shows good agreement. Furthermore a mesh convergence study was undertaken based on the number of elements per wavelength (hmax); results shown in Figure 2 confirm convergence for the reflection coefficient results.

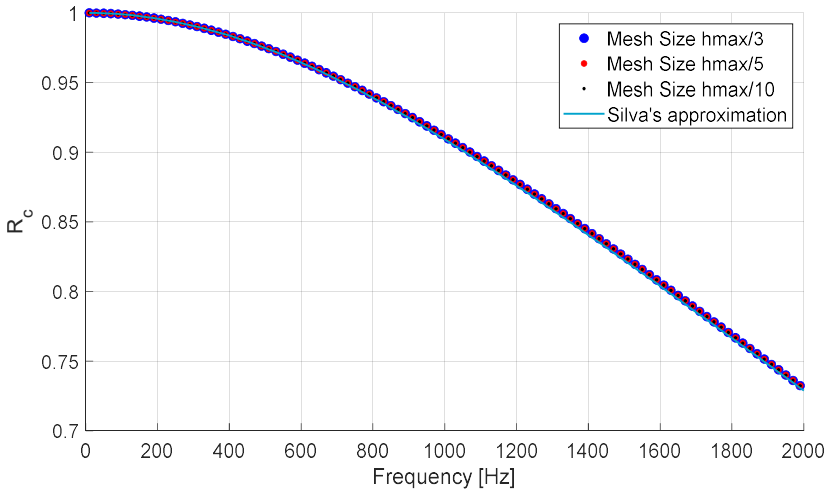

Figure 2 - Reflection coefficient vs frequency for an unflanged circular duct: numerical predictions from COMSOL for different mesh sizes are compared with Silva's approximation (F. Silva, 2009).

3 RESULTS AND DISCUSSION

3.1 Conical horn

The geometry of the conical horn and the material for the acoustic lining was found to strongly influence the reflection coefficient of the duct outlet. Figure 3 shows the reflection coefficient for the conical horn with different lengths, a throat diameter of $d = 0.05\,\mathrm{m}$ and a constant cone angle of $\theta = 40°$, as well as for two different poroacoustic materials. Also presented in Figure 3 for comparison is the approximation by Silva for an unflanged open ended duct as the "worse" case scenario. It is clear from the reflection coefficient that the poroacoustic material is an important factor, with the Durablanket showing lower reflection coefficients than the glass wool for the same geometry. Hence, based on the numerical simulations with the Miki model the air-flow resistivity is an important factor for determining the reflection coefficient, and the simulation results suggest improved anechoic performance for the material with the higher air-flow resistivity.

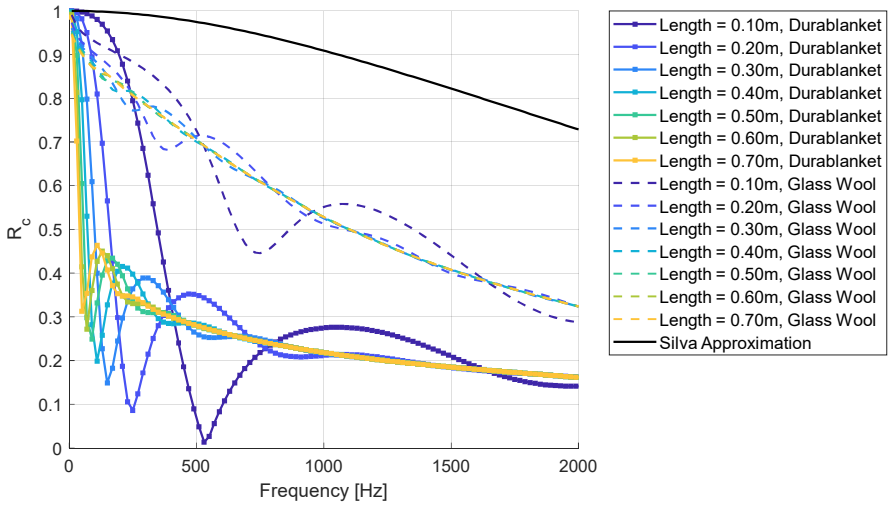

Figure 3 - Reflection coefficient against frequency for different horn lengths – a comparison between COMSOL glass and Durablanket. Horn angle is fixed at 40°, horn throat diameter is $d = 0.05\,\mathrm{m}$; length defined as in Figure 1b.

Regarding the length of the horn, the reflection coefficient results in Figure 3 show a trend for the two different air-flow resistivity cases. For the case with glass wool, it can be observed that as the length of the horn increases the ripple in reflection coefficient reduces and converges to a single curve. Hence, for a conical horn lined with glass wool material there is little benefit making the length of the conical horn greater than 0.4 m. The results presented in Figure 3 for the Durablanket clearly illustrate that the frequency of the first minimum in reflection coefficient is inversely proportional to length of the horn: approximately 500 Hz for L=0.1 m; 250 Hz for L = 0.2 m; to approximately 80 Hz for L = 0.7 m. It is important to note that there is also a local maximum at a frequency that is inversely to length. The ripple in the reflection coefficient reduces and converges to a single curve after the first local maxima in a similar way to the results for the conical horn lined with glass wool.

3.2 Catenoidal horn

Numerical simulations were conducted for the lined catenoid for different geometries, and this section will elaborate on these results. It should be noted that for the sake of brevity, only results for the Durablanket poroacoustic liner will be discussed, but investigations of different materials with different static air flow resistivities have been done, as well as studies using different poroacoustic models, such as the Delaney-Bazley model, modified Allard Champoux, and Miki model, which are all single parameter models using the static airflow resistivity.

Figure 4 quantifies the performance of the catenoid horn geometry by averaging R_c across the frequency range. It shows that average reflection coefficient decreases monotonically with increasing horn diameter, and for horn diameters greater than approximately 0.5 m the reflection coefficient also decreases monotonically with increasing length, which is consistent with Myers' analytical findings (Myers, 2012). At horn diameters less than 0.5 m, there appears to be an optimal horn length for the average reflection coefficient. This can be further analysed by looking at the reflection coefficient as a function of frequency for different lengths.

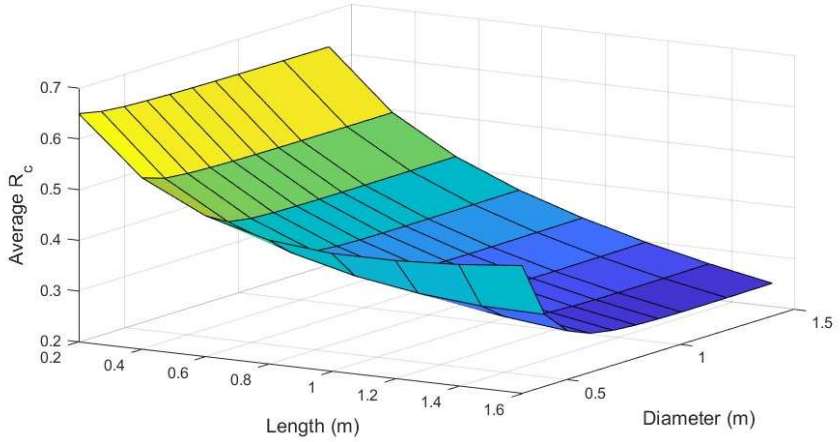

Figure 4 - Average R_c for different horn length and mouth diameter. Computed for Frequency=0-2200 Hz.

Figure 5 shows reflection coefficient for varying horn lengths and a constant mouth diameter of 0.3 m. As horn length increases, the first minimum in the reflection coefficient shifts towards lower frequencies from approximately 400 Hz to 50 Hz, and also increases in magnitude. This pattern is similar to that shown in Figure 3 for a conical horn. The ripple in the reflection coefficient tends to decrease with increasing frequency and with increasing length. An interesting result is that the 0.4 m length horn has the lowest average reflection coefficient in the frequency range 1000 – 2200 Hz, and average reflection coefficient in this frequency range increases from approximately 0.02 to close to 0.3 for as horn length increases from 0.6 m to 1.6 m.

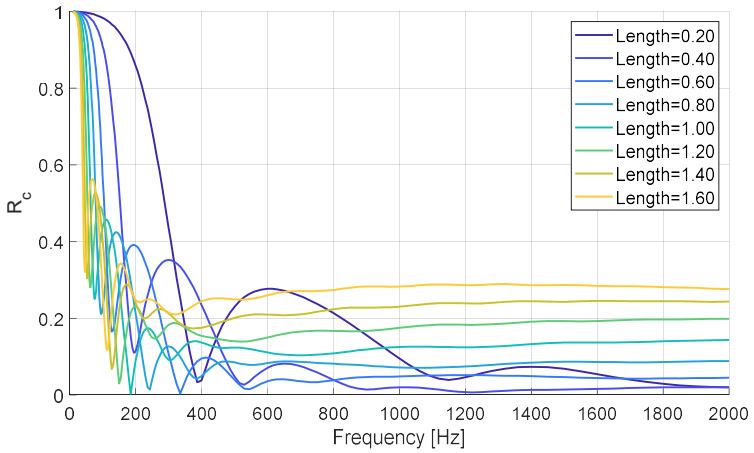

Figure 5 - Reflection coefficient across the frequency spectrum for different catenoidal horn lengths (mouth diameter=0.3 m).

A further observation of Figure 4 is the effect of increasing mouth diameter of the lined catenoidal horn. As the mouth diameter is increased, the magnitude of the average reflection coefficient drops significantly from diameters of 0.3 m to 0.8 m. It was found through numerical simulations that the acoustic field does not propagate as a plane wave through the poroacoustic layer of the horn, with much of the sound pressure constrained in the duct and

radiating as a narrow lobe. This effect was evident in the sound pressure fields, as shown in Figure 7. At the exit of the horn shown in Figure 7(a), there is an increase sound pressure observed at the interfacing surface between the poroacoustic lining and the air, which is indicative of reflections occurring at the interface. This effect is minimised by truncating the diameter of the horn as shown in Figure 7(b). Figure 8 shows that the truncated horn performs better than the full horn across most of the frequency spectrum. This could be attributed to the lower reflection at the liner-free air interface which is a smaller interface due to the truncation. This effect prompted further research into the reflections due to the liner itself through grazing flow and intermedia reflections, the findings of which were inconclusive and are not presented here.

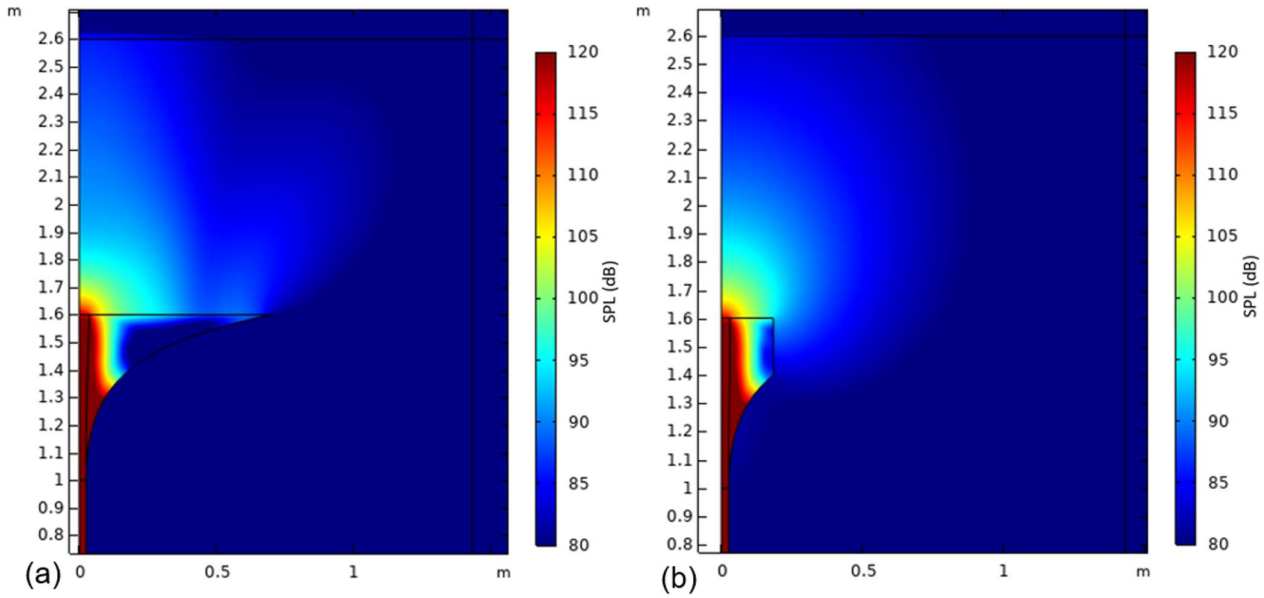

Figure 7 - (a) Sound Pressure Level for a full horn (b) Sound Pressure Level for a horn with a truncated diameter. Catenoidal section of both horns is identical with flare factor being determined by mouth diameter=1.4 m and length=0.6 m.

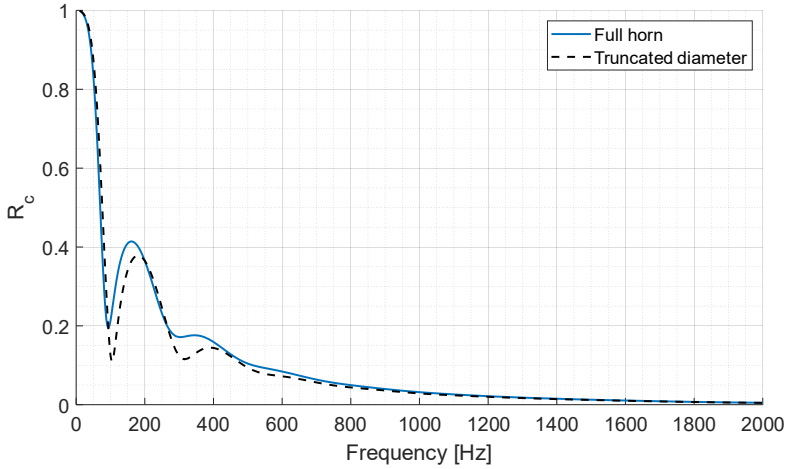

Figure 8 - Reflection coefficient across the frequency spectrum for a horn of mouth diameter=1.4 m and length=0.6 m, and the same horn with diameter truncated at length=0.4 m.

4 CONCLUSIONS

The research into the different geometries for the acoustically lined axisymmetric conical and catenoidal anechoic terminations provides detailed insights into minimizing the reflection coefficient. It was found that the geometry of the termination significantly affects the reflection coefficient across the frequency spectrum. Additionally, the type and amount of liner material plays an important role for conical horns; materials with higher flow-resistivity proved to be more effective in reducing the reflection coefficient.

The study highlighted the complexity of predicting the reflection coefficient across a broad frequency range for different geometry and static airflow resistivity, as these changes do not follow a simple trend. A finding of the numerical results is that anechoic terminations should ideally be long with a wide diameter, though truncating the diameter might also be beneficial. Future work should include studies of flow and temperature through the horn and how this influences the reflection coefficient. Furthermore, poroacoustic materials for this application should be investigated further as flow resistivity data for different materials was limited. Finally, this research should be extended to other horn geometries to verify that the catenoidal horn is the most effective. In this research, the catenoidal horn geometry and Durablanket liner material were found to be the most effective in minimizing the reflection coefficient.

REFERENCES

Bolleter, U., Cohen, R., & Wang, J. (1973). Design Considerations For An In-Duct Soundpower Measuring System. *Journal of Sound and Vibration*, 669-685.

COMSOL. (n.d.). *COMSOL application gallery*. (COMSOL) Retrieved January 11, 2024, from https://www.comsol.com/model/absorptive-muffler-1367

Donkin, S. (2020, 10 23). Development and qualification of an anechoic termination. University of Kentucky.

F. Silva, P. G. (2009). Approximation formulae for the acoustic radiation impedance of a cylindrical pipe. *Journal of Sound and Vibration, 322*, 255-263.

ISO5136:2003. (2003). *ISO 5136 Determination of sound power radiated into a duct by fans and other air-moving devices - In-duct method.* Switzerland: International Organization for Standardization.

Levine, H., & Schwinger, J. (1948). On the Radiation of Sound from an Unflanged Circular Pipe. *American Physical Society, 73*(4).

Munjal, M. L. (2014). *Acoustics of Ducts and Mufflers.* Chichester, West Sussex: John Wiley & Sons Ltd.

Myers, K. (2012). *Design of a Catenoidal Shaped Anechoic Termination.* Kalamazoo, Michigan: Western Michigan University.

Neise, W., & Arnold, F. (2001). On Sound Power Determination in Flow Ducts. *Journal of Sound and Vibration*, 481-503.

Wollherr, H. (1973). Akustische Untersuchungen an Radialventilatoren unter Verwendung der Vierpoltheorie. Berlin: Techn. Universität Berlin.

Xin, B., Yang, J., Jing, X., & Sun, X. (2018). Experimental and numerical investigation of anechoic termination for a duct with mean flow. *Applied Acoustics*, 213-221.